Tohoku J. Exp. Med., 2024, **264**, 193-202

Long Noncoding RNA GAS5 Contributes to *Mycoplasma pneumoniae* Pneumonia by Regulating NF-κB via miR-29c/HMGB1 Axis

Juhua Ji,[1,2,*] Fei Hong,[2,*] Yi Liu,[3] Xiaobin Chu,[2] Lei Song,[2] Meijun Zhu,[2] Yan Lu[2] and Chuangli Hao[1]

[1]Department of Respiratory Diseases, Children's Hospital of Soochow University, Suzhou, China
[2]Department of Pediatrics, The Second Affiliated Hospital of Nantong University, Nantong First People's Hospital, Nantong, China
[3]Department of Orthopedics, The Second Affiliated Hospital of Nantong University, Nantong First People's Hospital, Nantong, China

Mycoplasma pneumoniae pneumonia (MPP) poses a major threat to pediatric health. Our previous study suggested that GAS5 level was elevated in the peripheral blood of MPP children. However, the mechanism by which GAS5 regulates lung inflammation *Mycoplasma pneumoniae* (MP) infection-induced remains unknown. An MPP mouse model was constructed by MP intranasal injection to enrich for alveolar macrophage (AM). Mouse AM was stimulated using lipid-associated membrane proteins (LAMPs) to mimic an *in vitro* pneumonia model, and transfection was used to achieve specific knockdown or overexpression of target genes. GAS5 level was significantly increased in AM of the MPP mouse model, and significantly and positively related with the mRNA level of HMGB1, but no physical binding between GAS5 and HMGB1 proteins. miR-29c level was significantly decreased in AM of the MPP mouse model and negatively related with the HMGB1. We found the specific binding of GAS5 to miR-29c, and the specific binding of miR-29c to the HMGB1 mRNA 3'UTR. miR-29c mimic and knockdown of HMGB1 both significantly impeded LAMPs-induced apoptosis, IL-6 and TNF-α secretion, and the NF-κB activation. Ectopic expression of GAS5 counteracted the effect of miR-29c mimic, and miR-29c inhibitor counteracted the effect of HMGB1 knockdown. Furthermore, silencing of GAS5 significantly alleviated MPP-induced inflammation and pathological lung injury in the MPP mouse model. GAS5/miR-29c/HMGB1 is highly involved in inflammation and lung histopathological injury in MPP disease progression by regulating the NF-κB signaling pathway.

Keywords: GAS5; HMGB1; miR-29c; *Mycoplasma pneumoniae* pneumonia; NF-κB signaling pathway
Tohoku J. Exp. Med., 2024 December, **264** (4), 193-202.
doi: 10.1620/tjem.2024.J067

Introduction

Mycoplasma pneumoniae (MP) can cause upper and lower respiratory tract infections, and is the main pathogen responsible for pediatric community-acquired pneumonia (CAP) (Kumar 2018). Moreover, some recent cohort studies have indicated a decreasing trend in the age of onset of *Mycoplasma pneumoniae* pneumonia (MPP) (over 5 years of age), as well as an increase in the number of cases of MP-induced refractory pneumonitis and multisystemic complications, thus posing a major threat to pediatric health (Ocak et al. 2022).

Growth arrest-specific transcript 5 (GAS5) is a long noncoding RNA (lncRNA). Our previous study suggested that GAS5 level was elevated in peripheral blood from children with MPP and in lipid-associated membrane proteins (LAMPs)-stimulated macrophages compared to controls, and were significantly and positively correlated with TNF-α, IL-6, High-mobility group box protein 1 (HMGB1), p-p65, and p-IκBα expression (Ji et al. 2022). However, the

Received February 27, 2024; revised and accepted July 3, 2024; J-STAGE Advance online publication July 18, 2024
*These two authors contributed equally to this work and should be considered as equal first coauthors.
Correspondence: Chuangli Hao, Department of Respiratory Diseases, Children's Hospital of Soochow University, No. 92, Zhongnan Street, Wuzhong District, Suzhou, Jiangsu 215002, China.
e-mail: hcl_md@sina.com

possible molecular mechanisms by which GAS5 regulates lung inflammation due to MP infection remain unknown.

HMGB1 is a cytokine actively secreted by activated macrophages and other immune cells during the innate immune response (Abraham et al. 2000). Once released into the extracellular environment, HMGB1 acts as a potent pro-inflammatory cytokine, activating immune cells to produce other pro-inflammatory factors (e.g., TNF-α), which ultimately leads to epithelial leakage (Abraham et al. 2000). Direct exposure of the lungs to HMGB1 can lead to neutrophil infiltration, macrophage recruitment, inflammation and histopathological damage, which can be significantly ameliorated by the combination of anti-HMGB1 monoclonal antibodies in certain lung infections (e.g., *Pseudomonas aeruginosa*, H1N1 2009 influenza virus) (Entezari et al. 2012, Hatayama et al. 2019). A cohort study showed significantly higher levels of HMGB1 mRNA in bronchoalveolar lavage fluid (BALF) from MPP patients compared to healthy volunteers (Fan et al. 2022). In addition, HMGB1 mRNA levels were significantly higher in the peripheral blood of refractory MPP (RMPP) patients compared to non-refractory MPP, and HMGB1 was considered to be a potentially good diagnostic biomarker for RMPP (Ding et al. 2018). Surfactant protein A was reported to inhibit MP-induced dendritic cell maturation by regulating HMGB1 activity, thereby reducing lung inflammation (Ledford et al. 2010). These reports suggest that HMGB1 may highly involve in the inflammatory response and disease progression during MP infection.

Therefore, in this study, we will determine the critical roles of GAS5 and HMGB1 in the progression of MPP inflammation and reveal the molecular mechanisms involved in their roles by using an MPP mouse model and an *in vitro* pneumonia model induced by LAMPs.

Materials and Methods

Strain and LAMPs extraction

Mycoplasma pneumoniae strain (15531) was purchased from the ATCC, and maintained in SP-4 medium at 37°C and 5% CO_2. Titers were determined by colony formation assays and are expressed as colony forming units (CFU)/mL.

Invasive microorganisms express LAMPs on the cell surface that are the most potent elicitors of inflammatory responses to *Mycoplasma* infections. LAMPs can affect macrophage function to promote the production of proinflammatory factors. An *in vitro* pneumonia model induced by LAMPs can be well used to study (He et al. 2009; Wang et al. 2017). The LAMPs extraction was performed as previously reported (Shimizu et al. 2005). In brief, MP cultured to stationary growth phase were collected by centrifugation at 12,000 *g* for 10 min, and then resuspended with buffered saline (50 mM Tris-Cl, 1 mM ethyl acetate, 0.15 M NaCl, 2% Triton X-114, pH = 8.0). The resultant pellet was resuspended in 2 ml of PBS and layered upon a four-step sucrose gradient consisting of 5 ml of 60%, 7 ml of 52%, 7 ml of 48%, and 7 ml of 42% sucrose. The gradient was centrifuged in an SW28 rotor at 20,000 *g* for 15 min. Cells were harvested from the 48/52% interface, diluted in PBS, and washed free of sucrose by centrifugation. The viability of the cells assessed by colony counting was identical before and after the gradient purification. The purification of the organisms by density gradient centrifugation was essential because large amounts of protein precipitate co-sediment with mycoplasma in the initial centrifugation step and interfered with binding measurements and quantification of microbial protein content. After 1 h of incubation at 4°C, centrifugation was performed at 10,000 *g* for 20 min to separate the phases. The upper layer was discarded and the same volume of TBSE was added, which was vortexed and then incubated at 4°C for 10 min. The procedure was then repeated twice. Finally, 2.5 times the volume of ethanol was added and incubated at −20°C overnight. After centrifugation, the precipitate was resuspended and sonicated for 30 sec.

Animal and MPP model construction

C57BL/6 mice (female, 8 weeks old) confirmed to be viral and MP-free were provided by the Experimental Animal Center of Xuzhou Medical University. While under isoflurane anesthesia, each mouse was injected intranasally with 30 μL of MPP bacterial solution (1×10^7 CFU/mL, once/day for 3 days). On the fourth day, blood was collected from the orbital vein of the mice for mycoplasma extraction and detection according to the instructions of the MP Nucleic Acid Test Kit. Positive results were considered as successful modeling. After 10 days of normal feeding (mice were kept for a total of 14 days from the first day of MPP injection), the lung tissues were dissected for HE staining. After mice were euthanized, the trachea was exposed and the lungs were lavaged once with 1 mL of PBS through a 25-gauge needle inserted into the tracheal ring to obtain BALF. For alveolar macrophage (AM) enrichment, 1 mL of ice-cold HBSS solution supplemented with 0.6 mM EDTA was injected, and the lungs were washed three times to obtain BALF. AM was collected by centrifuging the BALF. The identification of collected AMs was performed based on flow cytometry with the antibodies against PE-Siglec F and PE-cy5.5-CD11c.

For GAS5 targeting, mice were injected intranasally for 7 consecutive days with 100 μl sh-GAS5 (1×10^8 TU/ml). All applicable international, national, and/or institutional guidelines for the care and use of animals were followed. This study was approved by Nantong First People's Hospital.

ELISA

Secretion levels of the IL-6, TNF-α, and HMGB1 were analyzed using the Mouse IL-6 ELISA Kit (BMS603HS, Thermo Fisher; Waltham, MA, USA), Mouse TNF-α ELISA Kit (BMS607-2HS, Thermo Fisher), and Mouse HMGB1 ELISA Kit (E-EL-M0676, Elabscience; Houston, TX, USA) according to the manufacturer's instruction.

RT-qPCR

Total RNA of cells was extracted using TRIzol reagent (Invitrogen; Carlsbad, CA, USA) and RNA Extraction Kit (CW0581S, CWBIO; Beijing, China), and reverse transcribed to cDNA using PrimeScript RT Reagent Kit (Takara, Japan). RT-qPCR was performed using SYBR Green I kit in the 7500 real-time PCR System (Applied Biosystems; Foster City, CA, USA) with the following thermal cycling program: 95°C predenaturation for 15 s, 40 cycles of 95°C denaturation for 10 s, 60°C annealing for 20 s, and 72°C extensions for 15 s. The expression levels of GAS5 and HMGB1 were normalized to the expression of GAPDH, and the expression levels of miRNAs were normalized to the expression of U6 using the $2^{-(\Delta\Delta Ct)}$ method. The primer sequences used are shown in Table 1.

Fluorescence in situ hybridization (FISH)-RNA

The collected AM from mouse were seeded into a 12-well plate placed with coverslips, and incubated for 12 h. Then, the cells were fixed with 3.7% formaldehyde solution for 10 min. Subsequently, the cells were covered with 70% ethanol solution and placed in 4°C environment for overnight permeabilization. The cells were contacted with hybridization solution spiked with the probe, and incubated overnight at 37°C in an incubator protected from light. The nuclei were stained with DAPI (5 ng/mL) and incubated for 30 min protected from light. Finally, the cells were imaged and analyzed under a confocal microscope.

RNA-immunoprecipitation (RIP)

AM obtained from mouse was suspended in lysis buffer. Anti-HMGB1 antibody was added to the cell lysate and incubated overnight at 4°C on a shaker. The prepared protein A/G magnetic beads were added to the antibody-incubated samples and incubated on a shaker at 4°C for 1 h. The precipitated complexes were collected by centrifugation. TRIzol solution was used to isolate the RNA in the precipitated complexes and further detected by PCR.

Table 1. The primers for PCR reaction.

Gene	Sequence	
HMGB1	Forward	TGAGGGACAAAAGCCACTCC
	Reverse	TTGGGAGGGCGGAGAATCA
GAS5	Forward	AGCGTCGGGTATGAGCTAAC
	Reverse	TGATTTCCTTCCGGCACGTC
GAPDH	Forward	TATGCACCTCACAACGCCAT
	Reverse	TGTACGGGTCTAGGGATGCT
miR-29c	Forward	CGCGTAGCACCATTTGAAAT
	Reverse	AGTGCAGGGTCCGAGGTATT
miR-145	Forward	CCAGTTTTCCCAGGAATCC
	Reverse	GAACATGTCTGCGTATCTC
miR-146a	Forward	CGCGCCTGTGAAATTCAGTT
	Reverse	AGTGCAGGGTCCGAGGTATT
miR-221	Forward	CGCGAGCTACATTGTCTGCTG
	Reverse	AGTGCAGGGTCCGAGGTATT
U6	Forward	GCTTCGGCAGCACATATACTA
	Reverse	CGAATTTGCGTGTCATCCTTG

Cells culture and transfection

Mouse alveolar macrophage MH-S cells were purchased from the Cell Bank of Chinese Academy of Sciences (Shanghai, China), and cultured in High glucose-DMEM (Gibco; Grand Island, NY, USA) with 10% FBS (Sigma-Aldrich; St. Louis, MO, USA) at 37°C and 5% CO_2. The siRNAs specifically targeting GAS5 and HMGB1, shRNA specifically targeting GAS5, miR-29c mimic and inhibitor were purchased from GenePharma (Shanghai, China). cDNA for GAS5 was cloned into pcDNA3.1 plasmid to construct the GAS5 expression plasmid. All RNA sequences and plasmids were transfected into cells using Lipofectamine 2000 reagent according to the manufacturer's instructions.

Dual luciferase reporter assay

The predicted binding sequences of wild-type (WT) or mutant (MUT) were amplified and cloned into the pGL3 base vector, respectively. The recombinant pGL3 plasmid and miR-29c mimic were co-transfected into MH-S cells using Lipofectamine 2000 reagent. After 48 h of incubation, cells were lysed with passive lysis buffer and luciferase activity was measured using the Dual Luciferase Reporter Analysis System and normalized to Renilla luciferase activity.

Flow cytometry to apoptosis

MH-S cells were seeded into a six-well plate at a density of 1×10^6 cells/well, cultured until 60% confluence and then transfected. After 6 h of transfection, the medium was changed to contain 5 μg of LAMPs. After 18 h of further incubation, cells were trypsin digested and resuspended in PBS. 200 μl of Annexin V-FITC conjugate was used to resuspend 5×10^5 cells, and 5 μl of Annexin V-FITC and 10 μl of PI staining solution were added sequentially. The mixture was incubated for 20 min in the dark. The cell populations were analyzed in the BD FACSAria II System, and results were analyzed with Flowjo 7.6 software.

Western blot

MH-S cells were seeded into a six-well plate at a density of 1×10^6 cells/well and cultured to 60% confluence for transfection. After 6 h of transfection, the medium was changed to contain 5 μg of LAMPs. After continuing the culture for 18 h, the cells were lysed on ice utilizing precooled strong RIPA solution containing protease inhibitors and phosphatase inhibitors. Cell lysates were centrifuged at 12,000 *g* for 10 min at 4°C to remove impurities and obtain protein supernatants. The concentration of protein samples was determined using a BCA assay kit. Aliquots of protein samples were heat denatured and spiked with 4x buffer,

separated by 12% SDS-PAGE, and electrotransferred to a PVDF membrane. Anti-p-p65 (ab32536, Abcam; Cambridge, MA, USA), anti-p-IκBα (AF5851, Beyotime; Beijing, China) and anti-β-actin (AF0003, Beyotime) were the primary antibodies, and HRP-labeled Goat Anti-Mouse IgG (A0216, Beyotime) and HRP-labeled Goat Anti-Rabbit IgG (A0208, Beyotime) were the second antibodies used in this study. The bands were visualized using the enhanced chemiluminescence detection system, and the intensity was analyzed using the ImageJ program.

Statistical analysis

All data were analysed using GraphPad Prism 8, and expressed as the mean ± standard deviation (SD). Comparison between the two groups was analyzed using the student's t-test while the comparison among multiple groups was analyzed by one-way analysis of variance followed by Tukey post hoc tests for multiple comparisons. Data are expressed as the mean ± SD. $P < 0.05$ were considered statistically significant.

Results

Expression of GAS5 and HMGB1 is significantly upregulated in AM in the MPP mouse model

We successfully constructed the MPP mouse model (Fig. 1A-C). The alveolar structures of mice in the control group were clear and there was no exudation in the alveoli, while the lung tissues of mice in the model group showed obvious pathological changes, which observed by HE staining (Fig. 1A). Described in detail, the alveolar lumen of the mice in the model group was narrowed, and inflammatory cell infiltration was seen in the interalveolar stroma, which was summarized as the appearance of interstitial pneumonia in the model group (Fig. 1A). The lung wet/dry weight ratio of mice in the model group was significantly higher than that of the control group (Fig. 1B). In addition, significantly increased levels of IL-6 and TNF-α were seen in the BALF of mice in the model group, as detected by ELISA (Fig. 1C).

During lung injury, AMs play a key role as they can orchestrate the initiation and resolution of inflammation. Hence, AMs were isolated from BALF for further analysis. The flow cytometry demonstrated the purity of AMs is greater than 98% (Supplementary Fig. S1A) and the morphology of isolated AMs was observed under microscope (Supplementary Fig. S1B). In the MPP mouse model, we detected significantly increased HMGB1 levels in BALF (Fig. 1D), as well as significantly increased HMGB1 expression in AM (Fig. 1E). GAS5 expression levels were also significantly elevated in AM of the model group and were mainly localized in the cytoplasm (Fig. 1F, G). The expression level of GAS5 was in a significant positive correlation with HMGB1 in AM of the model group (Fig. 1H). However, RIP experiments failed to detect physical binding and direct interaction between GAS5 and HMGB1 protein (Fig. 1I). To summarize, significantly upregulated expression of GAS5 and HMGB1, as well as a significant increase in the secretion of HMGB1, were observed in AM during MPP disease progression.

GAS5 promotes LAMPs-induced inflammation and apoptosis in an in vitro pneumonia model by targeting miR-29c

Recent studies have summarized miRNAs differentially expressed in MPP: miR-29c, miR-145, miR-146a, miR-221 (Gan et al. 2023). We similarly examined their expression levels in AM in control and MPP mouse models (Fig. 2A). miR-29c and miR-146a showed significant down-regulation of expression, miR-145 expression was up-regulated, and miR-221 lacked differential expression (Fig. 2A). Among the miR-29c and miR-146a with down-regulated expression, we further found that knockdown of GAS5 resulted in a significant increase in miR-29c levels, but had no effect on miR-146a levels in MH-S cells (Fig. 2B). Then, the miR-29c was overexpressed in MH-S cells by transfecting with miR-29c mimic (Fig. 2C). Based on the competing endogenous RNA (ceRNA) hypothesis, we also predicted a binding site for miR-29c on GAS5 (Fig. 2D). Dual luciferase reporter assays verified that GAS5 did bind to miR-29c through the putative binding site (Fig. 2E).

To further validate that GAS5 promotes MPP development by targeting miR-29c and down-regulating miR-29c levels, LAMPs were used to stimulate MH-S cells to induce an inflammatory response, mimicking an *in vitro* model of pneumonia, and transfection techniques were utilized to achieve overexpression of GAS5 in the cells (Fig. 2F). The expression of GAS5 was significantly elevated in MH-S cells after treatment with LAMPs (Supplementary Fig. S2A). LAMPs treatment significantly induced apoptosis of MH-S cells, as well as secretion of IL-6, TNF-α, and HMGB1 (Fig. 2G, H). These harmful effects induced by LAMPs were further aggravated by overexpressing GAS5 (Supplementary Fig. S2B-D). Consistent with previous findings, a significant up-regulation of p-p65 and p-IκBα expression were also found in LAMPs-treated MH-S cells (Fig. 2I, J). Furthermore, transfection with miR-29c mimic significantly hindered LAMPs-induced apoptosis, upregulation of IL-6 and TNF-α secretion, increased HMGB1 secretion and upregulation of p-p65 and p-IKBα expression (Fig. 2G-J). These results suggest that miR-29c plays a significant role in inhibiting inflammation in MPP progression, but its expression is significantly down-regulated during disease progression, possibly by GAS5. In LAMPs-treated MH-S cells, ectopic expression of GAS5 counteracted the role of miR-29c mimic (Fig. 2G-J). To summarize, GAS5 promoted inflammation and apoptosis by targeting miR-29c in an *in vitro* pneumonia model induced by LAMPs.

miR-29c inhibits LAMPs-induced inflammation and apoptosis by targeting HMGB1 mRNA in an in vitro pneumonia model

miR-29c level was negatively correlated with HMGB1 mRNA level in the AM of MPP mouse model (Fig. 3A). Subsequently, we predicted the binding site of miR-29c to

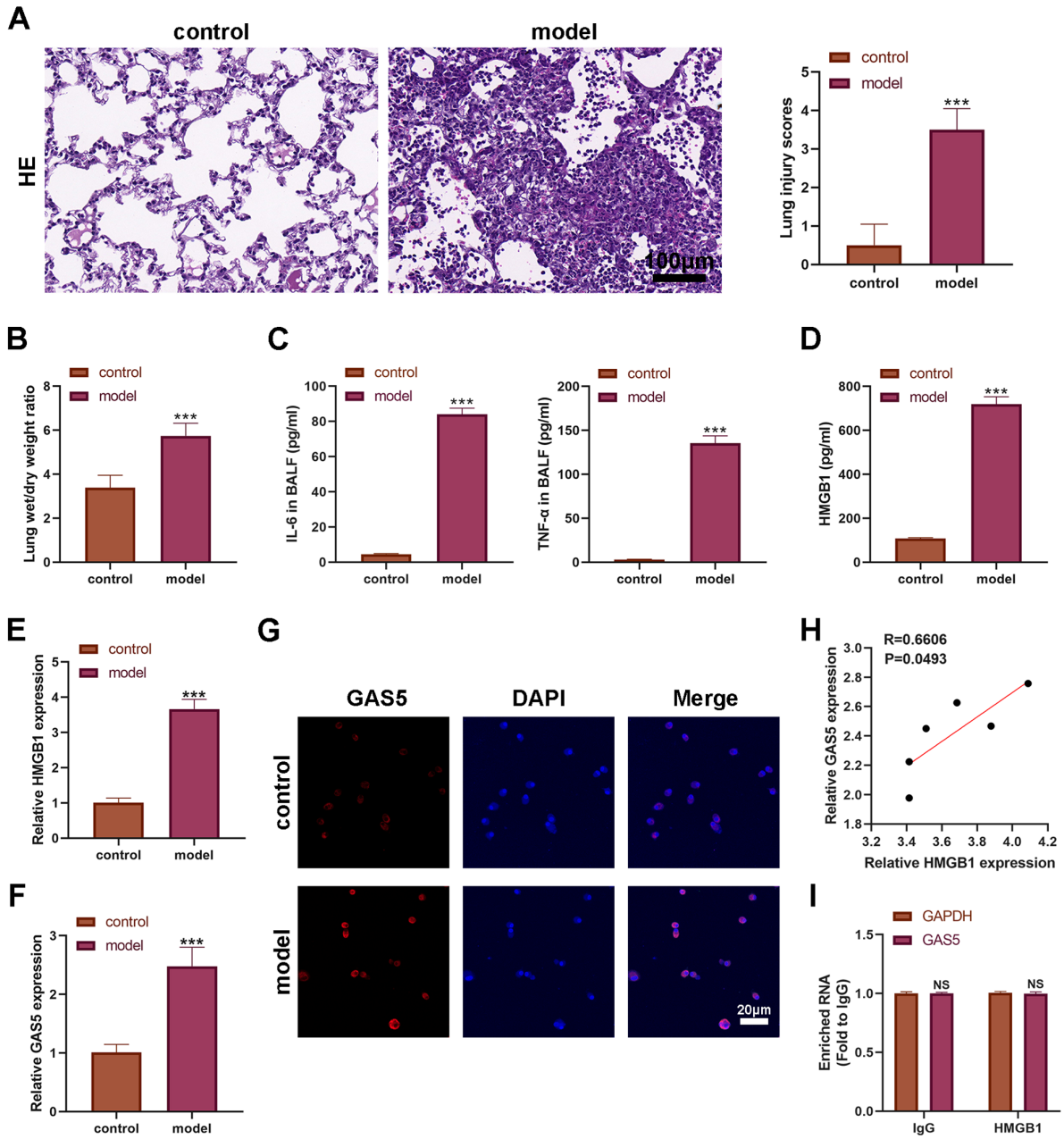

Fig. 1. Expression of GAS5 and HMGB1 is significantly upregulated in AM in the MPP mouse model.
A MPP mouse model was constructed. (A) The HE staining and injury score of lungs in the control and model mice. Scale bar: 100μm. (B)The lung wet/dry weight ratio of mice. The IL-6 and TNF-α levels (C) and HMGB1 levels (D) in the bronchoalveolar lavage fluid of mice, detected by ELISA. The expression of HMGB1 (E) and GAS5 (F) in alveolar macrophage (AM) of mice, detected by RT-qPCR. (G) The expression and location of GAS5 in AM of mice, detected by FISH. (H)The expression correlation analysis between GAS5 and HMGB1 in AM. (I) The RIP experiments result to detect physical binding between GAS5 and HMGB1 protein. ***P < 0.0001.

the 3'UTR region of HMGB1 mRNA (Fig. 3B), and confirmed their direct binding (Fig. 3C). Moreover, the binding site was consistent with the binding site of GAS5 to miR-29c. To verify that miR-29c inhibits inflammation in MPP progression by targeting HMGB1, we achieved knockdown of HMGB1 and miR-29c in LAMPs-stimulated mouse AM (Fig. 3D, E). Knockdown of HMGB1, as in the case of miR-29c mimic treatment, significantly hindered LAMPs-induced apoptosis, upregulation of IL-6 and TNF-α secretion, increased secretion of HMGB1 and upregulation of p-p65 and p-IκBα expression (Fig. 3F-I). And miR-29c inhibitor counteracted the HMGB1 knockdown (Fig. 3F-I). These results suggest that miR-29c inhibited LAMPs-induced inflammation and apoptosis in an *in vitro* pneumonia model by targeting HMGB1.

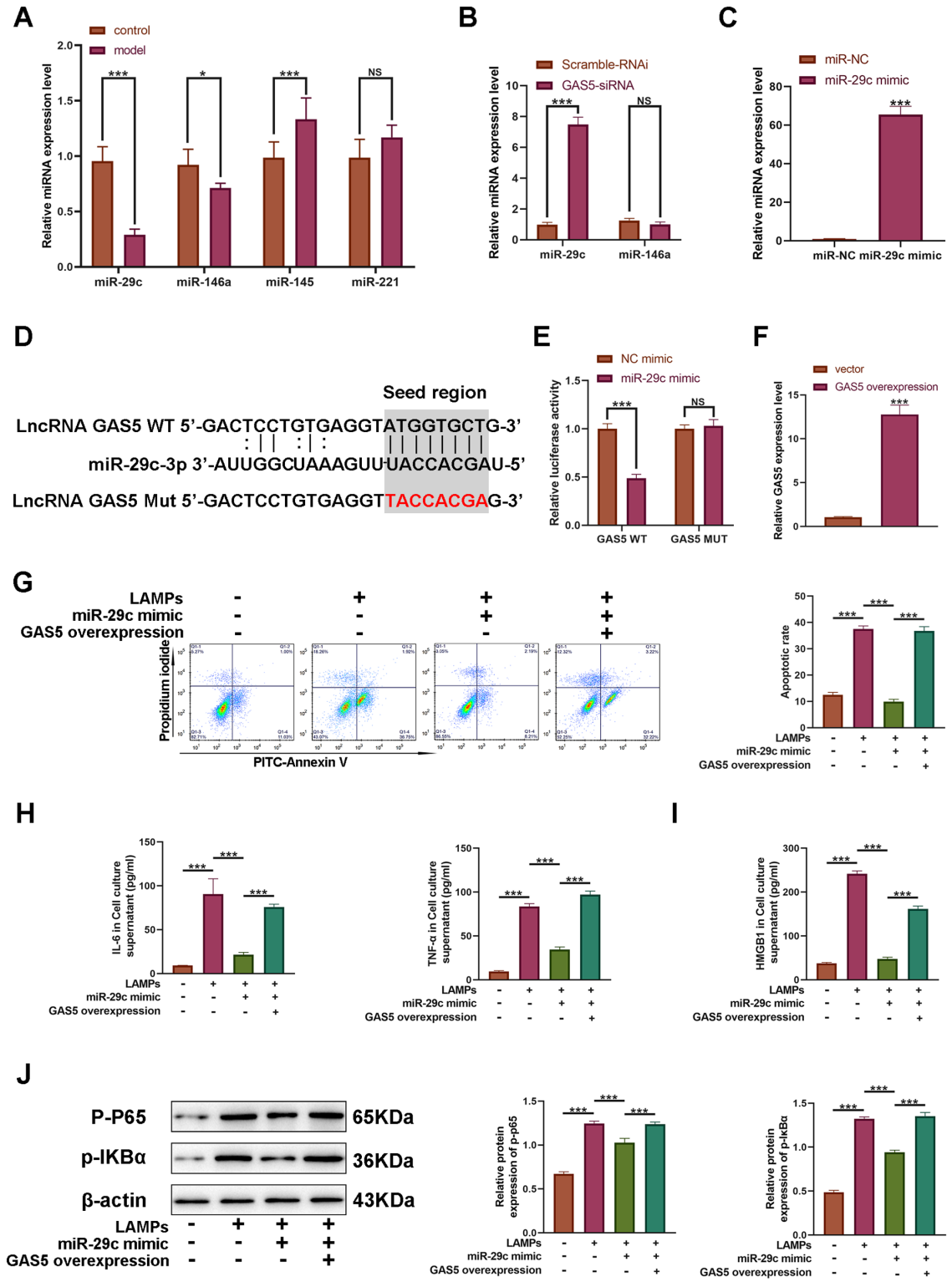

Fig. 2. GAS5 promotes LAMPs-induced inflammation and apoptosis in an *in vitro* pneumonia model by targeting miR-29c. (A) The expression levels of miR-29c, miR-145, miR-146a, and miR-221 in AM of control and MPP mouse were detected by RT-qPCR. (B) siRNA specifically targeting GAS5 (GAS5-siRNA) was transfected into MH-S cells, and the expression levels of miR-29c and miR-146a were detected. (C) miR-29c mimic was transfected into MH-S cells for upregulating miR-29c levels. (D) The predicted binding site for miR-29c on GAS5. (E) Relative luciferase activity. (F) GAS5 expression plasmid was transfected into MH-S cells for upregulating GAS5 expression. The apoptosis (G), IL-6 and TNF-α secretion (H), HMGB1 secretion level (I) and p-p65 and p-IκBα expression (J) of MH-S cells that were transfected by miR-29c mimic and GAS5 expression plasmid, and treated with LAMPs. *P < 0.05, ***P < 0.0001.

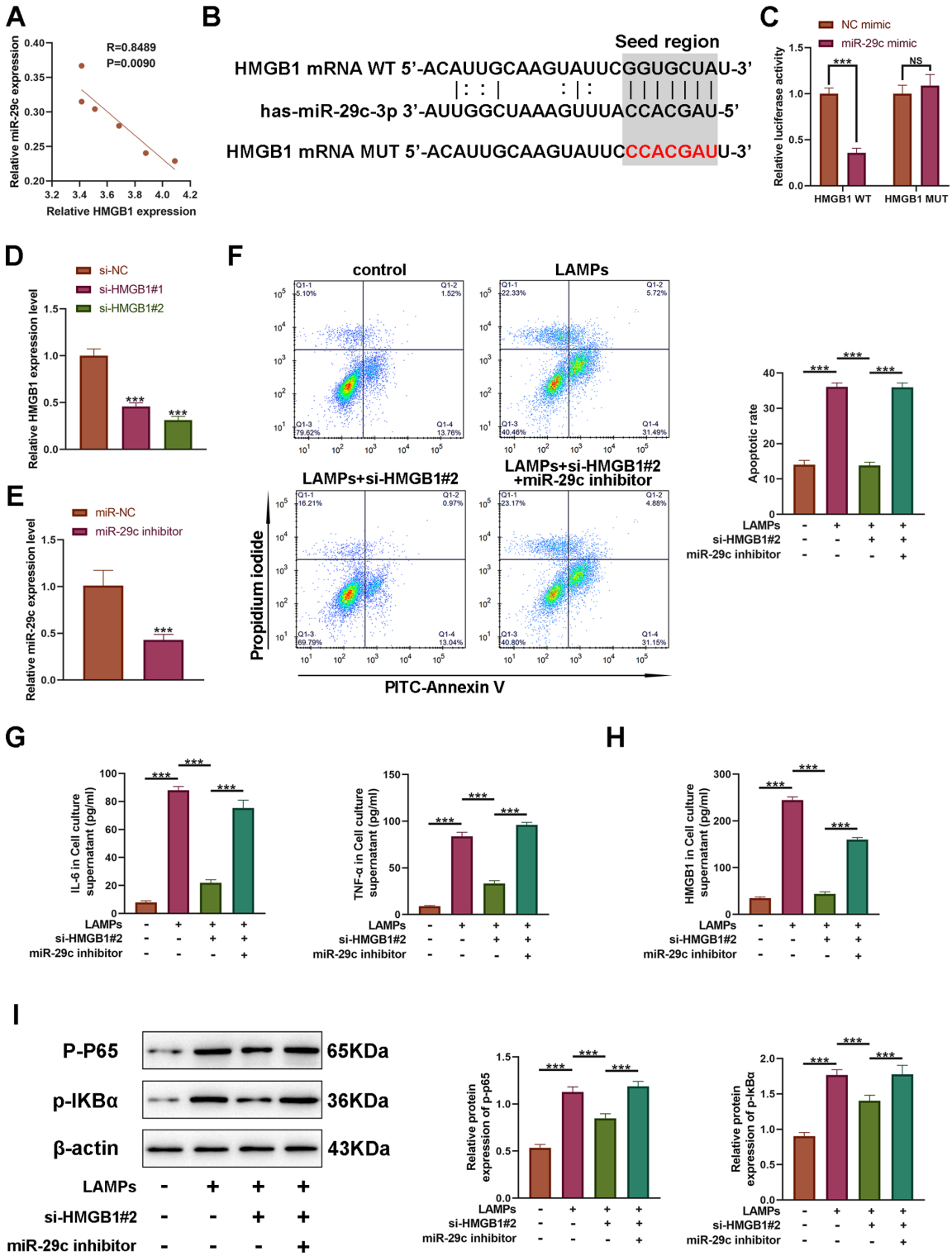

Fig. 3. miR-29c inhibits LAMPs-induced inflammation and apoptosis by targeting HMGB1 mRNA in an *in vitro* pneumonia model.

(A)The expression correlation analysis between miR-29c and HMGB1 in AM of MPP mouse. (B) The predicted binding site for miR-29c on HMGB1 mRNA 3'UTR. (C) Relative luciferase activity. (D) siRNAs specifically targeting HMGB1 (si-HMGB1) were transfected into MH-S cells for downregulating HMGB1 expression. (E) miR-29c inhibitor was transfected into MH-S cells for downregulating miR-29c levels. The apoptosis (F), IL-6 and TNF-α secretion (G), HMGB1 secretion level (H) and p-p65 and p-IκBα expression (I) of MH-S cells that were transfected by miR-29c inhibitor and si-HMGB1, and treated with LAMPs. ***P < 0.0001.

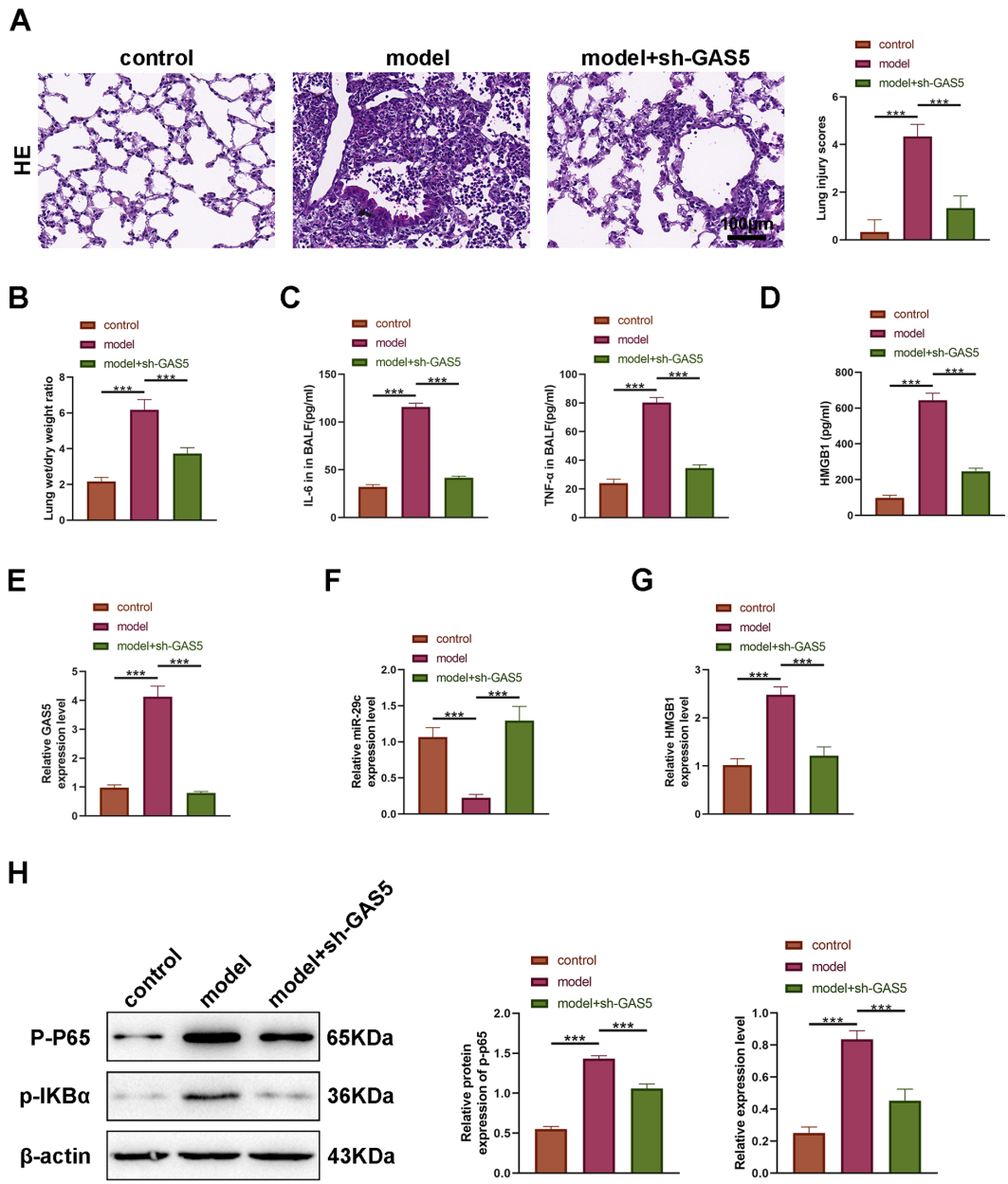

Fig. 4. Targeting GAS5 significantly attenuates the progression of pneumonia in the MPP mouse model. A MPP mouse model was constructed. (A) The HE staining and injury score of lungs. Scale bar: 100μm. (B)The lung wet/dry weight ratio of mice. The IL-6 and TNF-α levels (C) and HMGB1 levels (D) in the bronchoalveolar lavage fluid of mice, detected by ELISA. The expression of GAS5 (E), miR-29c (F), and HMGB1 (G) in AM of mice, detected by RT-qPCR. (I) The protein expression of p-p65 and p-IκBα in AM of mice, detected by western blot. ***P < 0.0001.

Targeting GAS5 significantly attenuates the progression of pneumonia in the MPP mouse model

To validate the effect of targeting GAS5 on alleviating inflammatory symptoms in MPP, we performed nasal injection of sh-GAS5 in the MPP mouse model. HE staining showed that sh-GAS5 significantly alleviated inflammatory cell infiltration as well as pathological changes caused by MPP (Fig. 4A). sh-GAS5 also significantly reduced the wet/dry weight ratio of lung tissue in the MPP mouse model, and the IL-6, TNF-α and HMGB1 levels in BALF (Fig. 4B-D). The expression levels of GAS5, miR-29c and HMGB1 in mouse AM were verified using RT-qPCR (Fig. 4E-G). Compared with the model group, sh-GAS5 significantly decreased the expression levels of GAS5 and HMGB1, and significantly increased the level of miR-29c (Fig. 4E-G). In addition, sh-GAS5 also affected the expression levels of p-p65 and p-IκBα (Fig. 4H). Taken together, targeting GAS5 significantly alleviated the progression of pneumonia in the MPP mouse model, and the effect involved the ceRNA action mechanism of GAS5/miR-29c/

HMGB1 as well as the NF-κB signaling pathway.

Discussion

In recent years, studies have begun to analyze lncRNAs that play a key role in MPP disease progression, although results are still scarce (Huang et al. 2021). Our previous study, based on the analysis of peripheral blood samples from MPP patients and an *in vitro* pneumonia model, demonstrated that GAS5 may highly involve in MPP progression (Ji et al. 2022). In this research, we further confirmed that GAS5 promoted MP infection-induced inflammatory response and lung histopathological damage using an MPP mouse model. Moreover, using the MPP mouse model, this study further demonstrated that targeting GAS5 significantly alleviated the inflammation and lung tissue injury caused by MP infection. Therefore, the research and development of small interfering RNAs, specific antibodies, small molecule inhibitors, or degradation agents targeting GAS5 will likely significantly improve the clinical treatment of MPP. In addition, this study revealed the key molecular mechanism by which GAS5 promotes MPP disease progression as a ceRNA targeting miR-29c/HMGB1.

According to recent reports, miR-29c is involved in neurogliogenesis in the retina and protein synthesis in skeletal muscle of animals, and also plays a role in multiple pathological processes such as Alzheimer's disease, Parkinson's, cancer, acromegaly, organ fibrosis, hyperglycemia, and viral infections (Cao et al. 2021; Korkmaz et al. 2021; Li et al. 2023). In addition to this, some studies have reported that serum miR-29c levels are significantly downregulated in children with MPP compared to healthy children, and the decrease is more pronounced in critically ill children (Li et al. 2019; Wang et al. 2023). The present study utilized a mouse model of MPP and an *in vitro* pneumonia model to demonstrate again the downregulation of miR-29c expression in the disease progression of MPP, and that treatment of miR-29c can alleviate inflammation. The downregulation of miR-29c may be due to the regulation by GAS5, but it does not exclude other expression regulation mechanisms, and further research on this is highly necessary. In addition, the action of miR-29c is mainly exerted by its target mRNAs, and it may target to regulate a variety of mRNAs. The present study revealed the targeting of miR-29c to HMGB1. Targeting of B7-H3 by miR-29c has also been reported (Li et al. 2019).

The NF-κB signaling pathway is involved in the expression regulation of various inflammatory response genes and highly involves in pneumonia caused by MP infection (Zhang et al. 2017). It has been reported that the lipoprotein component of MP can bind toll-like receptor 4 (TLR4), which then activates NF-κB, resulting in pneumonia (Shimizu et al. 2008). One lncRNA, NKILA, was found to physically bind IκBα, mask its phosphorylation motif, block and NF-κB activation, and ultimately reduce inflammatory cytokine secretion in MP-infected airway epithelial cells (Zhang et al. 2021). Another lncRNA, PACER was reported to physically bind to NF-κB p50 (Xu et al. 2022). The present study failed to reveal the physical binding and interaction of GAS5 with any of the key components of the NF-κB signaling pathway, what was revealed was the GAS5/miR-29c/HMGB1 axis. Normally, HMGB1 is mainly found in the nucleus. It has been reported that HMGB1 can act as a transcription factor and regulate the expression of IκBα (Liang et al. 2020). During stress, HMGB1 is acetylated or phosphorylated, then translocated into the cytoplasm and released into the extracellular space. Once released, HMGB1 becomes a damage-associated molecular pattern molecule that binds to the cell surface receptor TLR4, activating the downstream NF-κB signaling pathway and driving the inflammatory response (Lotze and Tracey 2005; Kang et al. 2014).

In this study, we found that MP infection leads to upregulation of GAS5 expression in AM which promotes disease progression of MPP through miR-29c/HMGB1 axis and NF-κB signaling pathway. However, from another point of view, the results of this study were limited to AM and did not analyze the differential expression of GAS5 in other host cells types of MP and in the major cell types of lung tissue, such as lung epithelial cells. This is a worthwhile direction for research. In addition, the present study did not further validate the role of miR-29c treatment in alleviating the pathologic damage of MPP using the MPP mouse model, which we will complete in the future. Last but not least, NF-κB activation has been proven to participate in lung MP clearance (Jiang et al. 2012), but whether the GAS5/miR29c/HMGB-1 pathway is involved in lung MP clearance remains poorly understood. This will also be explored in our future studies.

In conclusion, GAS5/miR-29c/HMGB1 plays an important role in inflammation and lung histopathological injury in MPP disease progression by regulating the NF-κB signaling pathway. Targeting GAS5, HMGB1 or NF-κB signaling pathway, and the addition of miR-29c may be beneficial for the treatment of MPP patients.

Acknowledgments

This work was supported by Research Project of Nantong Municipal Health Commission in 2023 (No. QNZ2023030 and No. MSZ2023013); Nantong Social Livelihood Science and Technology Plan Project in 2022 (No. MS22022026); Research Project of Nantong Municipal Health Commission in 2022 (No. MSZ2022011); and Nantong Basic Science Research and Social Livelihood Science and Technology Plan Project in 2022 (No. MSZ2022020).

Conflict of Interest

The authors declare no conflict of interest.

References

Abraham, E., Arcaroli, J., Carmody, A., Wang, H. & Tracey, K.J.

(2000) HMG-1 as a mediator of acute lung inflammation. *J. Immunol.*, **165**, 2950-2954.

Cao, Y., Tan, X., Lu, Q., Huang, K., Tang, X. & He, Z. (2021) MiR-29c-3p May Promote the Progression of Alzheimer's Disease through BACE1. *J. Healthc. Eng.*, **2021**, 2031407.

Ding, Y., Chu, C., Li, Y., Li, G., Lei, X., Zhou, W. & Chen, Z. (2018) High expression of HMGB1 in children with refractory Mycoplasma pneumoniae pneumonia. *BMC Infect. Dis.*, **18**, 439.

Entezari, M., Weiss, D.J., Sitapara, R., Whittaker, L., Wargo, M.J., Li, J., Wang, H., Yang, H., Sharma, L., Phan, B.D., Javdan, M., Chavan, S.S., Miller, E.J., Tracey, K.J. & Mantell, L.L. (2012) Inhibition of high-mobility group box 1 protein (HMGB1) enhances bacterial clearance and protects against Pseudomonas Aeruginosa pneumonia in cystic fibrosis. *Mol. Med.*, **18**, 477-485.

Fan, Y., Ding, Y., Li, Y., Zhang, D., Yu, M., Zhou, W.F. & Kong, X. (2022) Investigation of the relationship between community-acquired respiratory distress syndrome toxin and the high-mobility group box protein 1-toll-like receptors-myeloid differentiation factor 88 signaling pathway in Mycoplasma pneumoniae pneumonia. *Ital. J. Pediatr.*, **48**, 64.

Gan, T., Yu, J. & He, J. (2023) miRNA, lncRNA and circRNA: targeted molecules with therapeutic promises in Mycoplasma pneumoniae infection. *Arch. Microbiol.*, **205**, 293.

Hatayama, K., Nosaka, N., Yamada, M., Yashiro, M., Fujii, Y., Tsukahara, H., Liu, K., Nishibori, M., Matsukawa, A. & Morishima, T. (2019) Combined effect of anti-high-mobility group box-1 monoclonal antibody and peramivir against influenza A virus-induced pneumonia in mice. *J. Med. Virol.*, **91**, 361-369.

He, J., You, X., Zeng, Y., Yu, M., Zuo, L. & Wu, Y. (2009) Mycoplasma genitalium-derived lipid-associated membrane proteins activate NF-kappaB through toll-like receptors 1, 2, and 6 and CD14 in a MyD88-dependent pathway. *Clin. Vaccine Immunol.*, **16**, 1750-1757.

Huang, F., Fan, H., Yang, D., Zhang, J., Shi, T., Zhang, D. & Lu, G. (2021) Ribosomal RNA-depleted RNA sequencing reveals the pathogenesis of refractory Mycoplasma pneumoniae pneumonia in children. *Mol. Med. Rep.*, **24**, 761.

Ji, J., Song, L., Hong, F., Zhang, W., Zhu, M., Yang, X. & Hao, C. (2022) Highly Expressed lncRNA GAS5 in the Serum of Children with Mycoplasma pneumoniae Pneumonia and Its Effect on LAMPs-Induced Apoptosis and Inflammation. *Contrast Media Mol. Imaging*, **2022**, 7872107.

Jiang, D., Nelson, M.L., Gally, F., Smith, S., Wu, Q., Minor, M., Case, S., Thaikoottathil, J. & Chu, H.W. (2012) Airway epithelial NF-kappaB activation promotes Mycoplasma pneumoniae clearance in mice. *PLoS One*, **7**, e52969.

Kang, R., Chen, R., Zhang, Q., Hou, W., Wu, S., Cao, L., Huang, J., Yu, Y., Fan, X.G., Yan, Z., Sun, X., Wang, H., Wang, Q., Tsung, A., Billiar, T.R., et al. (2014) HMGB1 in health and disease. *Mol. Aspects Med.*, **40**, 1-116.

Korkmaz, H., Hekimler Ozturk, K. & Torus, B. (2021) Circulating miR-29c-3p is downregulated in patients with acromegaly. *Turk. J. Med. Sci.*, **51**, 2081-2086.

Kumar, S. (2018) Mycoplasma pneumoniae: A significant but underrated pathogen in paediatric community-acquired lower respiratory tract infections. *Indian J. Med. Res.*, **147**, 23-31.

Ledford, J.G., Lo, B., Kislan, M.M., Thomas, J.M., Evans, K., Cain, D.W., Kraft, M., Williams, K.L. & Wright, J.R. (2010) Surfactant protein-A inhibits mycoplasma-induced dendritic cell maturation through regulation of HMGB-1 cytokine activity. *J. Immunol.*, **185**, 3884-3894.

Li, H., Lv, J., Wang, J., Wang, H. & Luo, L. (2023) MiR-29c-3p represses gastric cancer development via modulating MEST. *Histol. Histopathol.*, **38**, 549-557.

Li, Q.L., Wu, Y.Y., Sun, H.M., Gu, W.J., Zhang, X.X., Wang, M.J., Yan, Y.D., Hao, C.L., Ji, W. & Chen, Z.R. (2019) The role of miR-29c/B7-H3/Th17 axis in children with Mycoplasma pneumoniae pneumonia. *Ital. J. Pediatr.*, **45**, 61.

Liang, W.J., Yang, H.W., Liu, H.N., Qian, W. & Chen, X.L. (2020) HMGB1 upregulates NF-kB by inhibiting IKB-alpha and associates with diabetic retinopathy. *Life Sci.*, **241**, 117146.

Lotze, M.T. & Tracey, K.J. (2005) High-mobility group box 1 protein (HMGB1): nuclear weapon in the immune arsenal. *Nat. Rev. Immunol.*, **5**, 331-342.

Ocak, M., Oz, F.N., Cinar, H.G. & Tanir, G. (2022) Clinical and radiologic manifestations of Mycoplasma pneumoniae infection in children. *Turk. J. Pediatr.*, **64**, 1031-1040.

Shimizu, T., Kida, Y. & Kuwano, K. (2005) A dipalmitoylated lipoprotein from Mycoplasma pneumoniae activates NF-kappa B through TLR1, TLR2, and TLR6. *J. Immunol.*, **175**, 4641-4646.

Shimizu, T., Kida, Y. & Kuwano, K. (2008) Mycoplasma pneumoniae-derived lipopeptides induce acute inflammatory responses in the lungs of mice. *Infect. Immun.*, **76**, 270-277.

Wang, J., Guo, C., Yang, L., Sun, P. & Jing, X. (2023) Peripheral blood microR-146a and microR-29c expression in children with Mycoplasma pneumoniae pneumonia and its clinical value. *Ital. J. Pediatr.*, **49**, 119.

Wang, Y., Wang, Q., Li, Y., Chen, Y., Shao, J., Nick, N., Li, C. & Xin, J. (2017) Mmm-derived lipid-associated membrane proteins activate IL-1beta production through the NF-kappaB pathway via TLR2, MyD88, and IRAK4. *Sci. Rep.*, **7**, 4349.

Xu, C., Deng, H., Liu, F., Zhao, D., Tang, H. & Gu, H. (2022) Long Non-Coding RNA PACER Regulates Mycoplasma pneumoniae-induced Inflammatory Response through Interaction with NF-kappaB. *Ann. Clin. Lab. Sci.*, **52**, 21-26.

Zhang, F., Zhang, J., Liu, F., Zhou, Y., Guo, Y., Duan, Q., Zhu, Y., Zhao, D. & Gu, H. (2021) Attenuated lncRNA NKILA Enhances the Secretory Function of Airway Epithelial Cells Stimulated by Mycoplasma pneumoniae via NF-kappaB. *Biomed. Res. Int.*, **2021**, 6656298.

Zhang, Q., Lenardo, M.J. & Baltimore, D. (2017) 30 Years of NF-kappaB: A Blossoming of Relevance to Human Pathobiology. *Cell*, **168**, 37-57.

Supplementary Files

Please find supplementary file(s);
https://doi.org/10.1620/tjem.2024.J067